

# Radicals as Probes of Ferroelectric Phase Transitions in EPR Investigations of Pyridinium Tetrafluoroborate

Ryszard Krzyminiewski, Aurelia Bielewicz-Mordalska, and Radoslaw Michal Kowalczyk

*Institute of Physics, Adam Mickiewicz University, 61-614 Poznan, Poland*

Received November 3, 1997; revised June 22, 1998

**This paper reports CW-EPR studies of pyridinium tetrafluoroborate undergoing solid–solid phase transitions at 240 and 205 K, of which the one occurring at the higher temperature was found to be paraelectric–ferroelectric. EPR spectra of  $\gamma$ -irradiated polycrystalline samples were taken at room temperature, at the liquid nitrogen temperature, and at temperatures ranging from 163 to 273 K in the cycles of cooling and heating. The radical appearing under the effect of  $\gamma$  irradiation was established to be formed by attachment of a hydrogen atom to the carbon atom C(2) in the pyridine ring. The unpaired electron was found to delocalize onto the pyridine ring. The  $g$  factor was established as 2.0021(4) and the values of the hyperfine splitting constants testify to the occurrence of an  $\alpha$ -type interaction,  $A_{\alpha} = 0.98(5)$  mT, of the unpaired electron with protons at the C(3), C(5), and N(1) positions, two  $\beta$ 1- and  $\beta$ 2-type interactions with the hydrogen nuclei at the C(2) position,  $A_{\beta 1} = 6.68(5)$  mT and  $A_{\beta 2} = 4.85(5)$  mT, and the interaction with the nitrogen nucleus at N(1),  $A_N = 0.86(5)$  mT. The complex character of the spectra obtained prompted us to employ computer analysis of the signals to enhance their resolution. Analysis of the temperature dependence of the line-width parameter of individual components of the pyridine radical spectrum shows that EPR together with the computer resolution enhancement method can be a useful method for studying the nature of phase transitions in pyridinium tetrafluoroborate.** © 1998 Academic Press

**Key Words:** electron paramagnetic resonance; phase transitions; molecular dynamics; pyridinium tetrafluoroborate; radicals.

## INTRODUCTION

Pyridinium salts have attracted much attention for a long time because of their interionic hydrogen bonding and the solid–solid phase transitions involving a change in the cation dynamics. A particularly interesting salt is pyridinium tetrafluoroborate as it undergoes a high-temperature phase transition of paraelectric–ferroelectric character at  $T_C = 240$  K and a low-temperature one at  $T = 205$  K. The temperature of the high-temperature transition was interpreted as the Curie point in this ferroelectric crystal.

Earlier NMR studies as well as Raman scattering measurements of the pyridinium salts revealed interesting behavior of the pyridine cation upon phase transition (1–3).

As with other pyridinium salts, pyridinium tetrafluoroborate

reveals orientational disorder of the pyridine cation and NMR studies disclosed the dynamical character of this disorder. The pyridinium cation, held rigidly in the crystal lattice in temperatures well below the phase transition, shows orientational disorder at room temperature (3–10). The pyridinium cation itself deserves particular attention because of its unique features: symmetry, planarity, and aromatic character.

Our study was undertaken mainly to check whether the free radicals generated by  $\gamma$  irradiation in pyridinium tetrafluoroborate can be used as probes in the studies of molecular dynamics and solid–solid phase transitions and if so, to determine the sensitivity of EPR parameters to changes in molecular dynamics and the solid–solid phase transitions.

The use of free radicals in investigations of molecular dynamics and phase transitions in molecular crystals by the CW-EPR method has been so far limited by serious difficulties in interpretation of the spectra stemming from the complex hyperfine structure of the experimental spectra which was a result of the unpaired electron interactions with many nuclei from its nearest neighborhood. This is why analysis of the hyperfine structure of EPR spectra has been rarely used in investigations of phase transitions. Moreover, interpretation of results obtained using the recent pulse techniques such as ESE is far from trivial. For instance, frequently it is difficult to find a correlation between the phase transition temperatures established on the basis of the critical behavior of parameters such as spin–lattice relaxation time  $T_1$  or phase memory time  $T_M$ , determined by the pulse methods, with those found from DTA and DSC examinations (11).

Since changes in dynamics of molecular crystals can be manifested not only in the width of the spectral lines but also in the hyperfine structure of the recorded spectra, we decided to check the usefulness of the standard CW-EPR method combined with the computer resolution enhancement method (CREM) for extracting more detailed information on the nature of phase transitions in complex molecular systems.

## EXPERIMENTAL

Pyridinium tetrafluoroborate was obtained by allowing pyridine to react with tetrafluoroboric acid. Pyridinium tetraflu-

**TABLE 1**  
**Basic Parameters of C<sub>5</sub>H<sub>6</sub>NBF<sub>4</sub> Single Crystals at 293, 230, and 4.5 K (2)**

Phase	Paraelectric	Ferroelectric ( $T_{PT} = 240$ K)	Ferroelastic ( $T_{PT} = 205$ K)
System	Rombohedral	Monoclinic	Monoclinic
Space group	$R\bar{3}m$	$C2$	$P2$
Lattice constants	$a = 5.669(1)$ Å $\alpha = 97.28(3)^\circ$	$a = 7.345(1)$ Å $b = 8.395(1)$ Å $c = 5.712(1)$ Å $\beta = 101.96(3)^\circ$	$a = 7.234(1)$ Å $b = 8.198(1)$ Å $c = 5.677(1)$ Å $\beta = 103.40(3)^\circ$
Number of atoms	$Z = 1$	$Z = 2$	$Z = 2$

oroborate crystallizes in the trigonal space group  $R\bar{3}m$ , with  $a = 5.626$  Å,  $\alpha = 97.51^\circ$ , and  $Z = 1$  (2, 6). Table 1 shows the crystal parameters.

EPR spectra were recorded on a Radiopan SE/X 2547 reflection bridge spectrometer working in the X band, applying a 100-kHz magnetic field modulation. Polycrystalline samples of pyridinium tetrafluoroborate (C<sub>5</sub>H<sub>6</sub>NBF<sub>4</sub>) were  $\gamma$ -irradiated at about 293 K using a <sup>60</sup>Co source with a 150-kGy dose.

Figure 1 shows the structural representation of a diamagnetic molecule (a) and radical (b) of pyridinium tetrafluoroborate with the atom numbering system.

EPR investigations were performed at the liquid nitrogen temperature and in a wide range of temperatures from 263 to 163 K in the cycles of cooling and heating. The temperature of the samples was maintained to within  $\pm 5$  K by a Radiopan 650R temperature controller; the temperature was measured by a copper–constantan thermocouple with an accuracy of  $\pm 5$  K.

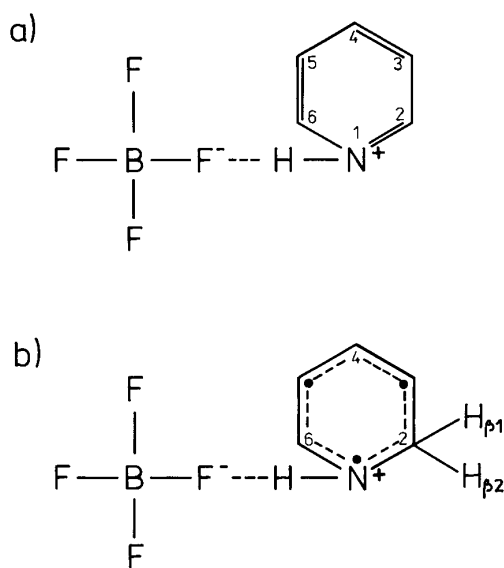


**FIG. 1.** Structural representation of a diamagnetic (a) and paramagnetic (b) molecule of pyridinium tetrafluoroborate with the atom numbering system.

## RESULTS AND DISCUSSION

For the continuous wave EPR studies we used irradiated polycrystalline samples of pyridinium tetrafluoroborate whose phase transition temperatures were independently confirmed by differential thermal analysis (DTA). The temperatures established by DTA were found to be the same as those for the nonirradiated diamagnetic material.

The EPR spectrum of polycrystalline samples of pyridinium tetrafluoroborate (C<sub>5</sub>H<sub>6</sub>NBF<sub>4</sub>) taken at room temperature is presented in Fig. 2a. It has a complex poorly resolved structure. To improve its resolution the spectrum was processed by a special program, RKU, designed for enhancement of spectral resolution (12, 13). The spectrum after processing is given in Fig. 2a'.

The EPR spectra taken at 243 and 203 K are presented in Figs. 2b and 2c, respectively. They were also processed by the

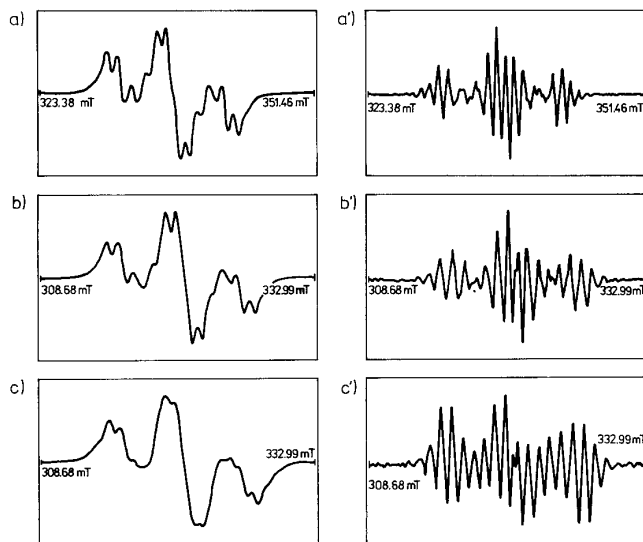


**FIG. 2.** Experimental EPR spectrum of pyridinium tetrafluoroborate taken in the X band at room temperature (a) and first derivative of the experimental spectrum after CREM processing (a'); (b) experimental spectrum taken at 243 K and (b') the spectrum of enhanced resolution, the first derivative; (c) experimental spectrum taken at 203K and (c') the enhanced resolution spectrum, the first derivative.

RKU program. The first derivatives of the experimental spectra after processing are given in Figs. 2b' and 2c'. The resonance lines of the spectrum are distributed symmetrically above and below the central resonance and are attributed to a radiation-induced stable radical exhibiting a complex hyperfine structure. The observed lines form a quartet, each component of which is split into quartets. Analysis of the hyperfine interactions between the unpaired electron, appearing after irradiation of this organic molecule, and the hydrogen nuclei provides information on  $\alpha$ - and  $\beta$ -type hyperfine interactions.

Formation of different possible types of radicals has been considered, assuming the possibility of attachment or abstraction of a hydrogen atom at different sites at the pyridine molecule, e.g., including attachment of a hydrogen atom to C(3). In such a case the unpaired electron would be delocalized mainly onto the C(2), C(4), and C(6) atoms but then no hyperfine interaction between the unpaired electron and nitrogen nucleus would be observed.

In order to verify the type of radical formed, we also studied pyridinium perchlorate ( $\text{PyClO}_4$ ) which differed from tetrafluoroborate by the geometry of the hydrogen bond. The studies of this salt revealed that the exchange of anion did not entail a change in the type of radical but affected only the strength of hyperfine interactions, i.e., changes in the delocalization of the unpaired electron on the pyridine ring (14). This fact confirms our supposition as to the type of radical formed.

An analysis of the hyperfine structure of  $\text{PyBF}_4$  spectra assuming a different location of the radical created by the ionizing radiation leads to the conclusion that the hydrogen atom is attached to the carbon atom C(2); see Fig. 1b. The values of the calculated hyperfine splitting constants testify to

the occurrence of an  $\alpha$ -type interaction,  $A_\alpha = 0.98(5)$  mT, of the unpaired electron with protons at the C(3), C(5), and N(1) positions and two  $\beta_1$ - and  $\beta_2$ -type interactions with the hydrogen nuclei at the C(2) position,  $A_{\beta_1} = 6.68(5)$  mT and  $A_{\beta_2} = 4.85(5)$  mT. Such high values of the splitting constants indicate a significant deformation of the ring during formation of the radical.

It was also found that the unpaired electron interacts with the nitrogen nucleus N(1),  $A_N = 0.86(5)$  mT. The  $g$  factor for this radical was found to be equal to 2.0021(4).

Our next objective was to study the changes in the spectral parameters of the EPR spectrum of pyridinium tetrafluoroborate complexes as a function of temperature. Preliminary measurements were performed in the range from 263 to 163 K, both on cooling and on heating of the sample. That there were no significant changes in the parameters of the spectrum taken at room temperature after completion of the cycle of cooling and heating proves that the pyridine radical is stable. However, the structure of the spectra changes considerably as a function of the sample temperature. Measurements at different microwave powers at selected temperatures permitted us to establish that changes in the experimental spectra were not caused by the sample saturation with the microwave radiation.

Analysis of the hyperfine structure and the width of particular spectral components of the spectra taken below 213 K was practically impossible, as indicated in Fig. 2c, so it would be absolutely pointless to draw any conclusions on the compound dynamics or its phase transitions from these spectra.

This fact prompted our effort to enhance their resolution.

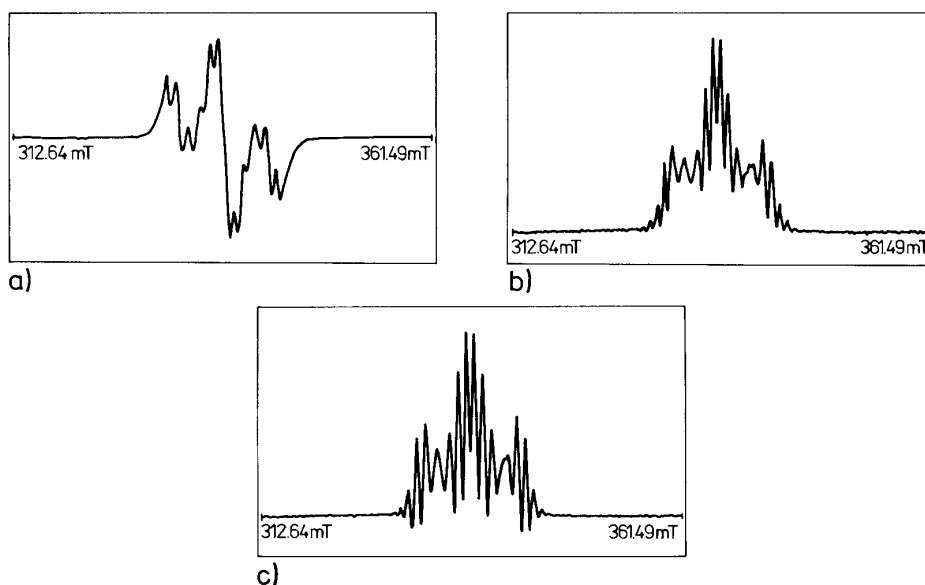


**FIG. 3.** (a) Experimental EPR spectrum of pyridinium tetrafluoroborate taken at room temperature; (b) the experimental spectrum after the resolution enhancement processing for the real width of the core, the absorption curve; and (c) the same experimental spectrum for a larger width of the core, the absorption curve.

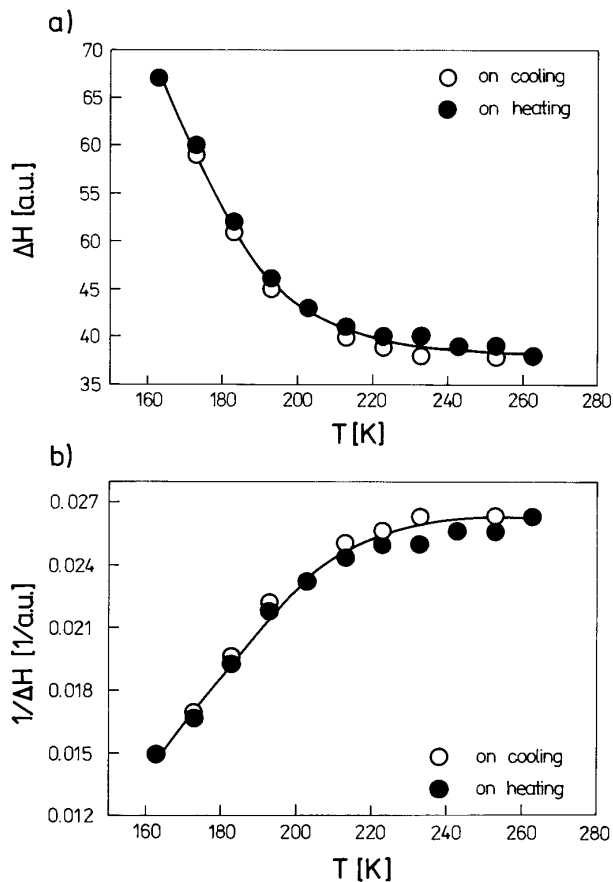


**FIG. 4.** (a) Temperature dependence of the linewidth parameter,  $\Delta H$  [a.u.]; and (b) temperature dependence of the inverse linewidth parameter,  $1/\Delta H$  [a.u.].

Attempts have been made to employ computer analysis for determination of the width of particular EPR spectrum components. Such an analysis has been performed using the RKU program based on the Fourier transform and the methods of convolution and deconvolution (CREM).

The shape of the spectrum is described by a function of the form

$$F(x) = \int_{-\infty}^{+\infty} K(x - x')\Psi(x')dx,$$

where the function  $\Psi(x')$  determines the positions and intensities of particular lines in the spectrum and  $K(x - x')$  is the so-called core, i.e., the function describing the shape and the width of individual lines. After performing the calculations several times for a given experimental spectrum, for various width parameters of the core, we were able to determine the actual widths of the lines forming the spectrum.

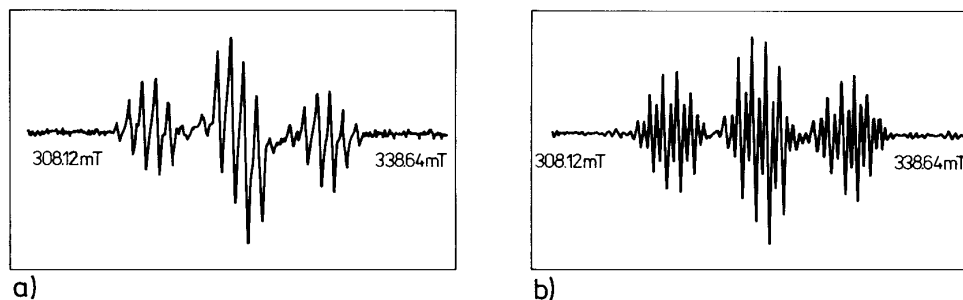
We have applied the RKU computer program not only to determine the hyperfine structure parameters (the number of lines and the resonance fields) but also to determine the width of individual components of the spectra (15).

Figure 3 shows three spectra of pyridinium tetrafluoroborate taken at room temperature: the experimental spectrum (a) and two other spectra obtained after RKU processing with the parameter equal to the real width (b) and for a greater value of this parameter (c). As shown in Fig. 3, if the core width assumed in the calculations was greater than the real one, computer processing gave an absorption curve with negative values of amplitude.

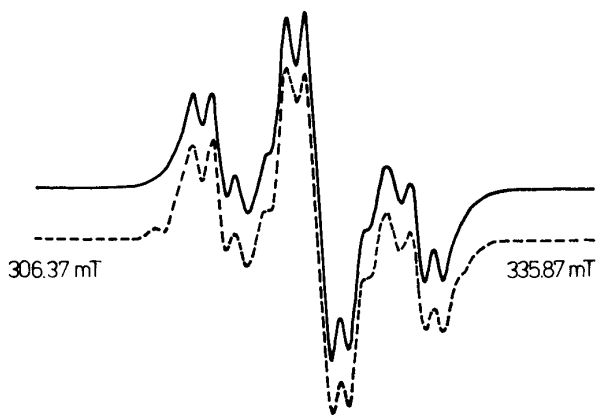
The RKU program is most effective if a given experimental spectrum consists of lines of the same or similar width and shape. The enhancement of resolution depends on the differences in the width of individual lines, and the positions and intensity ratios of all the lines in the converted spectrum undergo no change relative to the experimental one (12, 13).

Figure 4a presents the temperature dependence of the width parameter  $\Delta H$  [a.u.], equal to the core width, obtained in this way for certain lines of the experimental spectrum, while Fig. 4b shows the inverse of the width parameter ( $1/\Delta H$ ) [1/a.u.] as a function of temperature.

As follows from Fig. 4a, the width parameter increases with decreasing temperature and the experimental points can be approximated by an exponential dependence. However, in the range from 160 to 203 K they can be approximated by a linear function. The change from the linear to the exponential char-



**FIG. 5.** (a) Experimental spectrum of a single crystal of pyridinium tetrafluoroborate taken in the X band at room temperature when the single crystal was rotated in the  $ac$  plane and the  $a$  axis of the crystal made an angle of  $40^\circ$  with the magnetic field direction and (b) the first derivative of this experimental spectrum after CREM processing.



**FIG. 6.** Experimental EPR spectrum (—) recorded in the X band at 233 K and the simulated spectrum (- - -) obtained with the number of the lines and their positions as implied by RKU processing.

acter of the dependence takes place at the temperature corresponding to the low-temperature phase transition at 205 K.

Results of the preliminary EPR studies of  $\gamma$ -irradiated single crystals of pyridinium tetrafluoroborate performed at room temperature in the three orthogonal planes have confirmed our assumption as to the type of radical generated (19). Figure 5 shows the experimental spectrum of a single crystal of  $\text{PyBF}_4$  and the same spectrum after computer processing.

The measurements of the single crystal confirmed that the character of the temperature dependence of the width parameter was analogous to that obtained for a polycrystalline preparation, for different orientations of the single crystal in the magnetic field. Therefore, it can be concluded that the increase in the width parameter with decreasing temperature is not related to the anisotropy of the spectra of the polycrystalline material appearing as a consequence of the interaction averaging.

To confirm the results obtained earlier, a simulation of the EPR spectra was performed, Fig. 6. The calculation was performed for the positions and number of lines in the experimental spectrum taken after CREM processing. The variables in the simulation program were the amplitude and the linewidth. As shown in Fig. 6, the simulation gave a very good reproduction of the experimental spectrum.

The temperature dependencies of the width of selected lines of the simulated spectrum are shown in Fig. 7. Their character is similar to that of the analogous dependencies for the width parameter obtained from CREM processing. The discontinuity appearing at about 185 K can be related to the onset of rotation of an anion group at the temperature of the  $T_1$  relaxation time minimum determined for fluorine nuclei by NMR (3).

The hyperfine interactions were also found to change with temperature; e.g., the splitting of the extreme lines in the spectrum at 263 K was 16.24(5) mT while at 163 K it was 16.93(5) mT. However, to be able to perform a detailed anal-

ysis of a particular hyperfine interaction as a function of temperature, further studies are required.

The observed growing character of the temperature dependence of the linewidth can be explained as due to:

- (1) an increase in the dipolar interactions among radicals accompanying increasing strength of ordering interactions in the crystal;
- (2) unresolved superhyperfine structure; and
- (3) an increase in the anisotropy of hyperfine interactions and the anisotropy of the  $g$  value as a result of hindered rotation of molecules in the low-temperature phase.

Averaging of hyperfine interactions decreases with decreasing temperature; at and after the phase transition, the dynamics of the system changes and also, as indicated by the authors of (2–6), the hydrogen bond is affected. This in turn affects the character of the temperature dependence of the linewidth. The changes in the hydrogen bond have been confirmed by an increase in hyperfine interactions interpreted as due to the varied strength and direction of the bond between the anion and cation.

The authors of (10) suggest two models of ion motions

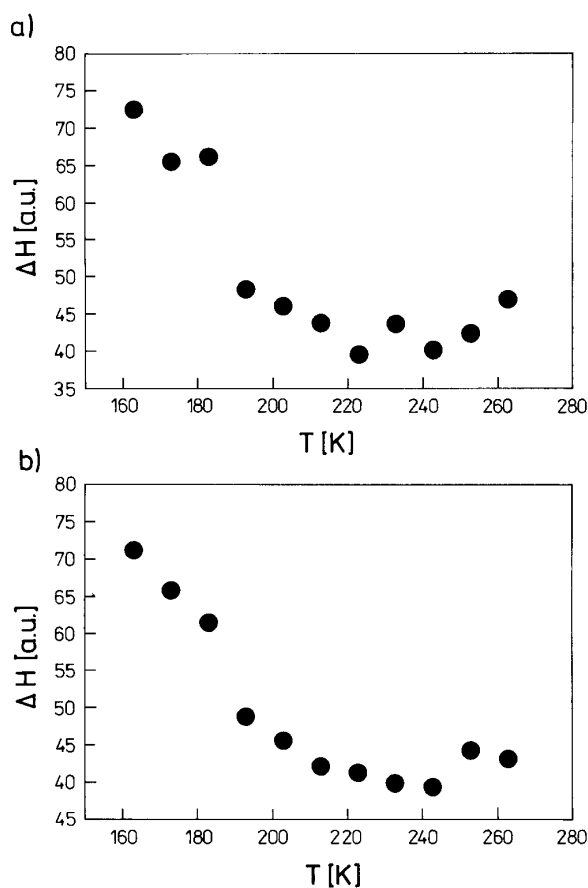


**FIG. 7.** Temperature dependence of the linewidth of two selected lines of the simulated spectrum shown in Fig. 6.

related to the in-plane  $60^\circ$  reorientational jumps of the cation about its pseudo-hexad axis between equivalent positions, as observed for other pyridinium salts (1, 3, 8, 14, 16–18), with simultaneous reorientation of the  $\text{BF}_4^-$  anion. The temperature dependencies of rotational correlation times for the cation and anion indicate a new kind of coupling in a distorted ionic crystal between the stochastic reorientation motions of cations and anions. In the phase transition a change in the hydrogen bond may play an essential role.

As follows from the results of our work, the application of the RKU computer program for enhancement of the EPR spectra resolution permitted determination of the width parameter of particular components of the spectrum as well as the constants of hyperfine splitting.

On the basis of the results obtained so far we can conclude that the pyridine radical formed upon irradiation can be used as a probe for detection of phase transitions. More detailed studies of the temperature changes of spectral parameters such as the width of particular components or the constants of hyperfine splitting of EPR spectra taken for polycrystalline samples and for single crystals of pyridinium tetrafluoroborate complex are expected to provide more information on the nature of phase transitions and molecular dynamics in this compound.

#### REFERENCES

1. J. Wasicki, W. Nawrocik, Z. Pajak, J. Natkaniec, and A. Belushkin, *Phys. Status Solidi A* **114**, 497 (1989).
2. P. Czarnecki, J. Wasicki, A. Kartusiak, C. Ecolivet, A. Girard, and A. Belushkin, *Physica B*, in press (1998).
3. J. Wasicki, Z. Pajak, and A. Kozak, *Z. Naturforsch. A* **45**, 33 (1990).
4. J. A. Ripmeester, *Can. J. Chem.* **54**, 3453 (1976).
5. Z. Pajak, K. Jurga, J. Wasicki, and W. Szczepanski, "Proceedings, 4th Spec. Coll. AMPERE," Leipzig, p. 198 (1979).
6. H. Hartl, *Acta Crystallogr. B* **31**, 1781 (1975).
7. R. F. Copeland, S. H. Conner, and E. A. Meyers, *J. Phys. Chem.* **70**, 1288 (1966).
8. W. Nawrocik, Z. Pajak, J. Wasicki, J. Natkaniec, and A. Belushkin, "Proceedings Conf. Mol. Cryst. 83," Vol. 1, p. 85 (1983). [In Polish]
9. C. Rerat, *Acta Crystallogr.* **15**, 427 (1962).
10. P. Czarnecki, W. Nawrocik, Z. Pajak, and J. Wasicki, *Phys. Rev. B* **49**, 1511 (1994).
11. W. Hilczer, S. K. Hoffmann, J. Goslar, J. Titt-Goc, and M. Augustyniak, *Solid State Commun.* **85**, 585 (1993).
12. R. Krzyminiewski, *Mol. Phys. Rep.* **6**, 174 (1994).
13. J. T. Masiakowski, R. Krzyminiewski, and J. Pietrzak, *Chem. Phys. Lett.* **116**, 387 (1985).
14. A. Bielewicz-Mordalska, R. Krzyminiewski, and Z. Kruczynski, "Proceedings, Int. Conf. Electron Spin Resonance in Electron Transfer and Organic Solids," Dresden, Germany, p. 7 (1995).
15. R. Krzyminiewski, A. Bielewicz, J. Kudynska, H. A. Buckmaster, and B. Brycki, *Physica B* **239**, 293 (1997).
16. J. A. Ripmeester, *J. Chem. Phys.* **85**, 747 (1986).
17. A. Kozak, M. Grottel, J. Wasicki, and Z. Pajak, *Phys. Status Solidi A* **143**, 65 (1994).
18. A. Kozak, M. Grottel, J. Wasicki, and Z. Pajak, *Phys. Status Solidi A* **141**, 345 (1994).
19. R. Krzyminiewski, A. Bielewicz-Mordalska, and R. M. Kowalczyk, "Proceedings, 2nd Int. Conf. Electron Paramagnetic Resonance of Radicals and Metal Complexes," Warsaw, Poland, p. 73 (1996).